

# Measurement of the complex polar magneto-optical Kerr effect using weak measurement

Tong Li<sup>Ⓧ</sup>,\* Yunhan Wang<sup>Ⓧ</sup>,\* Yinghang Jiang<sup>Ⓧ</sup>, and Zhiyou Zhang<sup>Ⓧ</sup>†  
*College of Physics, Sichuan University, Chengdu, Sichuan 610065, China*

Sijie Zhang<sup>Ⓧ</sup>  
*College of Physics, Sichuan University, Chengdu, Sichuan 610065, China and  
 Guizhou University of Engineering Science, Bijie, Guizhou 551700, China*

Lan Luo<sup>Ⓧ</sup>‡  
*the National Key Laboratory of Optical Field Manipulation Science and Technology,  
 Chinese Academy of Sciences, Chengdu 610209, China  
 Key Laboratory of Science and Technology on Space Optoelectronic Precision Measurement,  
 Chinese Academy of Sciences, Chengdu, Sichuan 610209, China and  
 Institute of Optics and Electronics, Chinese Academy of Sciences, Chengdu, Sichuan 610209, China*  
 (Dated: September 27, 2023)

Polar magneto-optical Kerr effect (PMOKE) is one of the most widely being applied magneto-optical Kerr effects (MOKE) due to the induced complex MOKE signal, consisting of the Kerr rotation angle and the ellipticity, is very sensitive to the magnetization component perpendicular to the magnetic surface. However, the Kerr rotation angle and the ellipticity invariably coexist and pose a challenge in their separation. This dual presence plays a pivotal role in defining the light intensity detected, ultimately restricting the advancements in the measurement precision. In this paper, we propose a weak measurement (WM) scheme to measure the complex MOKE in the pure polar configuration. Unlike the traditional MOKE or WM method using a quarter-wave-plate to measure the Kerr rotation angle and the ellipticity separately, we realize the simultaneous measurement of these two parameters in a single WM process using two new pointers, which possesses a larger linear response region compared with the previous amplified shift pointer. The measurement precision for the complex PMOKE angle reaches to  $10^{-4}$  deg in our experiment. Besides, the complex magneto-optical constant  $Q$  is also calculated. This work is of great significance for the measurement of the complex PMOKE with high efficiency, ultra-precision, low cost, and is an important attempt to obtain complex physical quantities using WM.

## I. INTRODUCTION

The magneto-optical Kerr effect (MOKE) refers to the phenomenon that when a beam of polarized light incident on the surface of the magnetic medium, the polarization state of the reflected light is changed. It can be represented by two parameters, the Kerr rotation angle  $\theta_K$  and the ellipticity  $\varepsilon_K$ . There are three cases of MOKE depending on the direction of the magnetization relative to the surface. Firstly, the polar magneto-optical Kerr effect (PMOKE) is found for the case where the magnetization is perpendicular to the surface. Secondly, the longitudinal magneto-optical Kerr effect (LMOKE) is found for the case where the magnetization is parallel to the surface and in the plane of incidence. Thirdly, the transverse magneto-optical Kerr effect (TMOKE) is found for the case where the direction of the magnetization is parallel to the surface and perpendicular to the plane of incidence [1, 2]. For oblique incidence, when the magnetization direction is arbitrary, any of the three Kerr effects may contribute to the detected MOKE signal. Thus the Kerr signal is mixed. For the quantitative analysis, it is important to distinguish each Kerr

effect. For example, to measure the magnetization component that perpendicular to the film plane, the pure PMOKE is usually distinguished by employing normal incident polarized light [3, 4], where TMOKE or LMOKE is absent. Except for the magnetism measurement, PMOKE has also been widely applied in the development of magnetic domain imaging, magneto-optical recording, etc., because it is very sensitive to the magnetization component of the surface normal.

In recent years, some studies used weak measurement to detect the MOKE signal [5–8], which has the advantages of higher precision and lower cost. Weak measurement is a technique for the measurement of high-precision parameters by amplifying the observed signals. It consists of the processes of pre-selection, weak coupling, and post-selection. It was first proposed by Aharonov, Albert, and Vaidman in 1988 [9]. Since weak measurement improves the signal-to-noise ratio significantly and has extremely high sensitivity, it has been used in the detection of beam shift [10–13], frequency [14], optical phases [15–17], chirality [18, 19], chemical reaction processes [20, 21], angular rotations [22], refractive index [23, 24], optical conductivity [25], and phase transition process [26].

Studies of the measurements of MOKE based on weak measurement are mostly realized by employing the polarization state of the beam as the pre- and post-selection state, and the spin splitting induced by the sample as the weak coupling. However, the spin splitting only exists with the oblique inci-

\* These authors contributed equally to this work.

† Corresponding author: zhangzhiyou@scu.edu.cn

‡ Corresponding author: naloul@163.com

dent light. Thus it is hardly to measure the pure PMOKE. What's more, to characterize the complex MOKE,  $\theta_K$  and  $\varepsilon_K$  are usually measured separately by using and adjusting the angle of a quarter-wave-plate both in the traditional MOKE setup [27] and weak measurement method [28]. However, it not only decreases the measurement efficiency, but also brings an extra error given by the separate measurement processes.

In this work, we propose a method to measure the complex MOKE signal in the pure polar configuration using weak measurement. The polarized light beam is reflected normally from the magnetic film before reaching to the surface of a glass prism obliquely. The spin splitting is induced by the glass prism, which is regarded as the weak coupling. We then introduce two new pointers calculated by the amplified shift and the intensity of the light to characterize the pure complex PMOKE. We realize the simultaneous measurement of  $\theta_K$  and  $\varepsilon_K$ . Compared to the traditional methods of separately measuring these two parameters, it greatly improves the efficiency and the precision. In our experiment, the complex magneto-optical constant  $Q$  is also calculated. This work has value in the measurement and the application of the complex PMOKE.

## II. THEORY

Considering an incident Gaussian beam with the polarization state of  $|\psi_0\rangle$  reaching a magnetic surface from a nonmagnetic medium, as shown in Fig. 1, the state of the reflected light can be described as

$$|\psi_r^1\rangle = \mathfrak{R}_1 |\psi_0\rangle, \quad (1)$$

$\mathfrak{R}_1$  is the magneto-optical Fresnel reflection matrix and can be represent as

$$\mathfrak{R}_1 = \begin{bmatrix} r_{pp} & r_{ps} \\ r_{sp} & r_{ss} \end{bmatrix}, \quad (2)$$

where  $r_{pp}$ ,  $r_{ps}$ ,  $r_{sp}$  and  $r_{ss}$ , the Fresnel coefficients corresponding to the magnetic medium, are expressed by [2]

$$\begin{aligned} r_{pp} &= \frac{n_1 \cos \theta_0 - n_0 \cos \theta_1}{n_1 \cos \theta_0 + n_0 \cos \theta_1} - \frac{2in_0n_1 \cos \theta_0 \sin \theta_1 m_x Q}{n_1 \cos \theta_0 + n_0 \cos \theta_1}, \\ r_{ss} &= \frac{n_0 \cos \theta_0 - n_1 \cos \theta_1}{n_0 \cos \theta_0 + n_1 \cos \theta_1}, \\ r_{ps} &= \frac{in_0n_1 \cos \theta_0 (\cos \theta_1 m_z Q - \sin \theta_1 m_y Q)}{(n_1 \cos \theta_0 + n_0 \cos \theta_1) (n_0 \cos \theta_0 + n_1 \cos \theta_1) \cos \theta_1}, \\ r_{sp} &= \frac{in_0n_1 \cos \theta_0 (\cos \theta_1 m_z Q + \sin \theta_1 m_y Q)}{(n_1 \cos \theta_0 + n_0 \cos \theta_1) (n_0 \cos \theta_0 + n_1 \cos \theta_1) \cos \theta_1}. \end{aligned} \quad (3)$$

In the above expressions,  $n_0$ ,  $n_1$ ,  $\theta_0$  and  $\theta_1$  are the incidence angle, the complex refractive angle calculated by Snell's law, refractive index of the nonmagnetic medium, and that of the magnetic medium, respectively.  $m_x$ ,  $m_y$  and  $m_z$  are the direction cosines of the magnetization  $\mathbf{M}$ , and are related to TMOKE, LMOKE and PMOKE, respectively.  $Q = Q_0 \exp(-iq)$  is the complex magneto-optical constant, whose

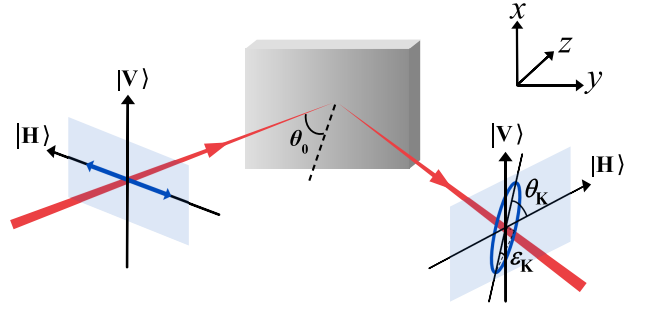


FIG. 1: Diagram of a Gaussian beam incident on the surface of a magnetic film.  $x$ ,  $y$ ,  $z$  are the directions parallel to the surface and perpendicular to the plane of the incident light, parallel to the surface and in the plane of incidence, and perpendicular to the surface, respectively.

magnitude  $Q_0$  is proportional to the magnetization intensity [1] and  $q$  is its phase factor.

For incidence with horizontal polarization  $|\psi_0\rangle = |H\rangle$ , the state of the reflected light is described as

$$\begin{aligned} |\psi_r^1\rangle &= \mathfrak{R}_1 |H\rangle \\ &= r_{pp} |H\rangle + r_{sp} |V\rangle \\ &= \frac{r_{pp}}{\sqrt{2}} \left[ (|+\rangle + |-\rangle) - i \frac{r_{sp}}{r_{pp}} (|+\rangle - |-\rangle) \right] \\ &\approx \frac{r_{pp}}{\sqrt{2}} \left[ e^{-i\theta_K - \varepsilon_K} |+\rangle + e^{i\theta_K + \varepsilon_K} |-\rangle \right]. \end{aligned} \quad (4)$$

Here,  $|+\rangle = (|H\rangle + i|V\rangle)/\sqrt{2}$  and  $|-\rangle = (|H\rangle - i|V\rangle)/\sqrt{2}$  are the left- and the right-circular polarization states (i.e., the spin basis).  $|H\rangle$  and  $|V\rangle$  denote the horizontal and the vertical polarized components, respectively. The complex MOKE signal can be described as [2]

$$\Theta_K = \frac{r_{sp}}{r_{pp}} = \frac{\cos \theta_0 (m_y \tan \theta_1 + m_z)}{\cos(\theta_0 + \theta_1)} \frac{in_0n_1Q}{n_1^2 - n_0^2}, \quad (5)$$

where  $\Theta_K = \theta_K - i\varepsilon_K$  is the complex magneto-optical Kerr angle,  $\theta_K$  and  $\varepsilon_K$  are the Kerr rotation angle and the ellipticity, respectively. From Eq. (5), we can see when the incident beam is oblique to the magnetic film plane, both  $m_y$  and  $m_z$  contribute to  $\Theta_K$ , so LMOKE and PMOKE are mixed in the detected signal [8]. Here, we extract the signal of the pure PMOKE by employing the normal incident light. In this case, Eq. (5) can be simplified to

$$\Theta_K = \frac{in_0n_1Qm_z}{n_1^2 - n_0^2}. \quad (6)$$

It also can be seen from Eq. (5) that, the smaller the incident angle, the larger the PMOKE signal. Different from the PMOKE signal, the spin splitting shows the opposite dependence with the incident angle  $\theta_0$  when  $\theta_0$  is less than the Brewster's angle [29]. And when  $\theta_0 = 0$ , the spin splitting is zero. (The theoretical detail is shown in Appendix A.) Thus

it is hardly to realize the measurement of the pure PMOKE when employ the spin splitting of the sample as the weak coupling.

Considering the light undergoes a second reflection from a glass surface obliquely with the incident angle of  $\theta_i$ , the spin splitting exists. We employ the spin splitting induced by the prism as the weak coupling. The state of the reflected light is described as

$$\begin{aligned} |\psi_r^2\rangle &= \exp(-i\delta\hat{\sigma}_3k_y)\mathfrak{R}_2|\psi_r^1\rangle \\ &= \exp(-i\delta\hat{\sigma}_3k_y)|\psi_{\text{pre}}\rangle, \end{aligned} \quad (7)$$

where  $\hat{\sigma}_3 = |+\rangle\langle+| - |-\rangle\langle-|$  represents the spin operator of a photon [10],  $\delta = (1 + r_s/r_p) \cot \theta_i/k$  is the spin splitting of  $|H\rangle$  incidence, and  $\exp(-i\delta\hat{\sigma}_3k_y)$  represents the spin-orbit coupling.  $|\psi_{\text{pre}}\rangle = \mathfrak{R}_2|\psi_r^1\rangle$  is regarded as the pre-selection. And

$$\mathfrak{R}_2 = \begin{bmatrix} r_p & 0 \\ 0 & r_s \end{bmatrix} \quad (8)$$

is the Fresnel reflection matrix of dielectric surface.

The post-selection state is given by

$$|\psi_{\text{post}}\rangle = |V\rangle = -\frac{i}{\sqrt{2}}(|+\rangle - |-\rangle). \quad (9)$$

Therefore, the final wave function is

$$|\Phi\rangle = \exp(-ik_y^2z/2k) \langle\psi_{\text{post}}|\exp(-i\delta\hat{\sigma}_3k_y)|\psi_{\text{pre}}\rangle|\phi\rangle. \quad (10)$$

$\exp(-ik_y^2z/2k)$  denotes the free evolution of the system, where  $z$  is the free propagation distance, and  $k_y$  is the wave vector in the direction  $y$ .  $|\phi\rangle = \int dk_y |k_y\rangle (w/\sqrt{2\pi})^{1/2} \exp(-w^2k_y^2/4)$  is the transverse distribution of the Gaussian beam, where  $w$  is the beam waist. And

$$\begin{aligned} A_w &= \frac{\langle\psi_{\text{post}}|\hat{\sigma}_3|\psi_{\text{pre}}\rangle}{\langle\psi_{\text{post}}|\psi_{\text{pre}}\rangle} \\ &= \frac{r_p \sinh 2\varepsilon_K - i \sin 2\theta_K}{r_s \cos 2\theta_K - \cosh 2\varepsilon_K} \end{aligned} \quad (11)$$

is the weak value.

The amplified shift of the beam

$$\begin{aligned} \Delta|_{\theta_k, \varepsilon_k} &= \frac{\langle\Phi|\hat{y}|\Phi\rangle}{\langle\Phi|\Phi\rangle} = \frac{\int_{-\infty}^{+\infty} \Phi^*(k_y) i\partial k_y \Phi(k_y) dk_y}{\int_{-\infty}^{+\infty} \Phi^*(k_y) \Phi(k_y) dk_y} \\ &\approx \frac{z}{R_0} \frac{2r_s r_p \delta \sin 2\theta_K}{[r_s^2 - r_p^2 + e^{k_0\delta^2/R_0}(r_s^2 + r_p^2)] \cosh 2\varepsilon_K - [r_s^2 + r_p^2 + e^{k_0\delta^2/R_0}(r_s^2 - r_p^2)] \cos 2\theta_K} \end{aligned} \quad (12)$$

is the pointer.  $R_0 = kw^2/2$  is the Rayleigh distance. The theoretical relationship between the amplified shift  $\Delta$  and the complex PMOKE is shown in Fig. 2(a). It can be seen that the role of  $\varepsilon_K$  is almost ignored when the complex PMOKE is weak enough. Thus, the pointer  $\Delta$  can be used to measure weak  $\theta_K$ .

However,  $\Delta$  is nearly linear with  $\theta_K$  only when  $\theta_K$  is smaller than  $10^{-2}$  deg, so the linear measurement region is limited in practical application. What's more, it is hardly to provide the information about  $\varepsilon_K$  when we employ  $\Delta$  as the only pointer.

To obtain more information, we introduce the intensity of the light as the second pointer:

$$\begin{aligned} I|_{\theta_k, \varepsilon_k} &\propto \langle\Phi|\Phi\rangle = \int_{-\infty}^{+\infty} \Phi^*(k_y) \Phi(k_y) dk_y \\ &\propto [r_s^2 - r_p^2 + e^{k_0\delta^2/R_0}(r_s^2 + r_p^2)] \cosh 2\varepsilon_K - [r_s^2 + r_p^2 + e^{k_0\delta^2/R_0}(r_s^2 - r_p^2)] \cos 2\theta_K. \end{aligned} \quad (13)$$

It is also related to MOKE but dependent nonlinearly with  $\theta_K$  or  $\varepsilon_K$ .

We then use the modified shift  $\Delta'$ , which is linear to  $\theta_K$  in the whole area, and the relative intensity change of  $\eta$ , as the

two new pointers, to characterize the pure complex PMOKE:

$$\Delta'|_{\theta_k} = \frac{I|_{\theta_k, \varepsilon_k}}{I|_{\theta_k=0, \varepsilon_k=0}} \Delta \approx \frac{2zr_s}{k\delta r_p} \theta_K, \quad (14)$$

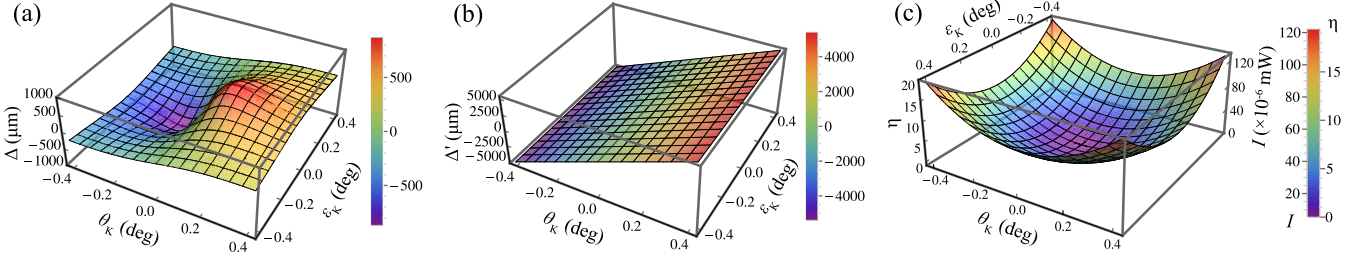


FIG. 2: Theoretical dependence of the pointers on the parameters of the complex PMOKE. (a) The amplified shift  $\Delta$  changing with  $\theta_K$  and  $\epsilon_K$ . (b) The modified shift  $\Delta'$  is only a function of  $\theta_K$  and independent of  $\epsilon_K$ , which shows a higher dynamic measurement range with wider consistent sensitivity compared with the standard weak measurement scheme (c) relative intensity change as well as the post-selected intensity changing with  $\theta_K$  and  $\epsilon_K$ .

$$\eta|_{\theta_K, \epsilon_K} = \frac{I|_{\theta_K, \epsilon_K} - I|_{\theta_K=0, \epsilon_K=0}}{I|_{\theta_K=0, \epsilon_K=0}} \approx \frac{r_s^2 w^2}{r_p^2 \delta^2} (\theta_K^2 + \epsilon_K^2), \quad (15)$$

where  $I|_{\theta_K=0, \epsilon_K=0}$  is the post-selected intensity of the light without MOKE. Here, we use the approximation conditions of  $\theta_K \ll 1$ ,  $\epsilon_K \ll 1$ , and  $|\delta/w| \ll 1$ . The theoretical dependencies of the two new pointers and the complex PMOKE parameters are shown in Fig.2(b) and Fig.2(c). It can be seen that the value of  $\Delta'$  is mainly dependent on  $\theta_K$ , while  $\eta$  and  $I$  are determined by both of  $\theta_K$  and  $\epsilon_K$ . It is worthy noted that the values of all the pointers are at the minimum when MOKE is absent.

### III. EXPERIMENT

The measurement system is shown in Fig. 3. The light source is a He-Ne laser with a wavelength of 632.8 nm, which passes through a half-wave plate (HWP) to adjust the intensity of the light. Next, the light beam passes through a polarizer P1 to obtain the initial state  $|\psi_0\rangle = |H + \alpha\rangle$ , where  $\alpha$  is a slight compensate angle used for adjusting the initial  $\Delta$  to be 0. After passing through the beam splitter (BS), the beam reaches to the surface of the magnetic thin film normally and the magnetic field is applied in a direction perpendicular to the surface of the film. After that, the reflected light is focused by a lens L1 and then reflected obliquely from the BK-7 glass prism. The incident angle of  $\theta_i = 40^\circ$  is kept throughout the experiment. With this photon wavelength and incident angle, the refractive index of the glass prism is 1.51.  $r_p$  and  $r_s$  are 0.122 and  $-0.282$ , respectively. A lens L2 is used to collimate the beam before the post-selection. The focal lengths of the lenses L1 and L2 are 50 mm and 250 mm, respectively. A polarizer P2 is used to prepare  $|\psi_{\text{post}}\rangle$  as the post-selection state. The detection of the reflected beam is finally carried out using a CCD photodetector.

A Ni-Fe film with the thickness of 30 nm that depositing on the silicon substrate is prepared for the experiment. During the measurement, the applied magnetic field  $H$  is changed from 0 to 0.45 T with steps of 0.05 T. At each value of  $H$ , the amplified shift and the intensity of the beam are recorded 30 times

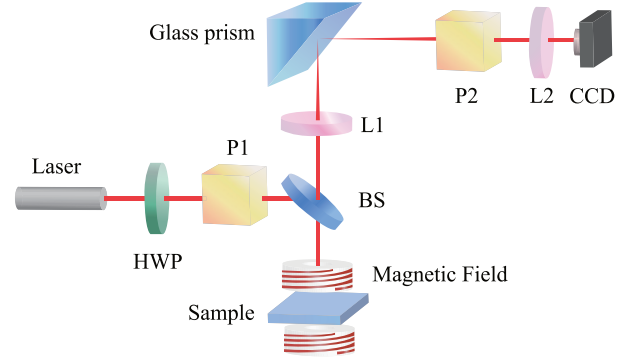


FIG. 3: Setup for the detection of the pure PMOKE. The light source is a He-Ne laser (wavelength=632.8 nm), HWP is a half-wave plate, P1 and P2 are Glan laser polarizers, BS is a beam splitter, L1 and L2 are the lenses with the focal lengths of 50 mm and 250 mm respectively, CCD is a charge-coupled device.

with intervals of 1 second by the CCD. The measurement results of  $\Delta$  and  $I$  are shown in Fig. 4(a) and 4(b). It can be seen that both  $\Delta$  and  $I$  increase with the increase of  $H$ , due to the increase of  $\theta_K$  and  $\epsilon_K$ , which is consistent with our theory. Fig. 4(c) and 4(d) show the two new pointers calculated by the experiment results. Here,  $I|_{\theta_K=0, \epsilon_K=0} = 5.7 \times 10^{-6}$  mW is determined by measuring the minimum value of  $I$  while changing  $H$ , under the condition of  $|\psi_0\rangle = |H\rangle$  and  $|\psi_{\text{post}}\rangle = |V\rangle$ .

Furthermore, we can describe the complex PMOKE with the two new pointers. According to Eq.(14) and Eq.(15), the expressions of  $\theta_K$  and  $\epsilon_K$  can be given by

$$\theta_K|_{\Delta'} = \frac{k\delta r_p}{2zr_s} \Delta' + \alpha, \quad (16)$$

$$\epsilon_K|_{\Delta', \eta} = \sqrt{\frac{r_p^2 \delta^2}{r_s^2 w^2} \eta - \left(\frac{k\delta r_p}{2zr_s} \Delta'\right)^2}. \quad (17)$$

Where the derivation can be seen in Appendix B. In this experiment,  $\alpha = 0.035$  deg. Thus, we can calculate the dependence of the complex MOKE and  $H$ . The results of  $\theta_K$  and  $\epsilon_K$

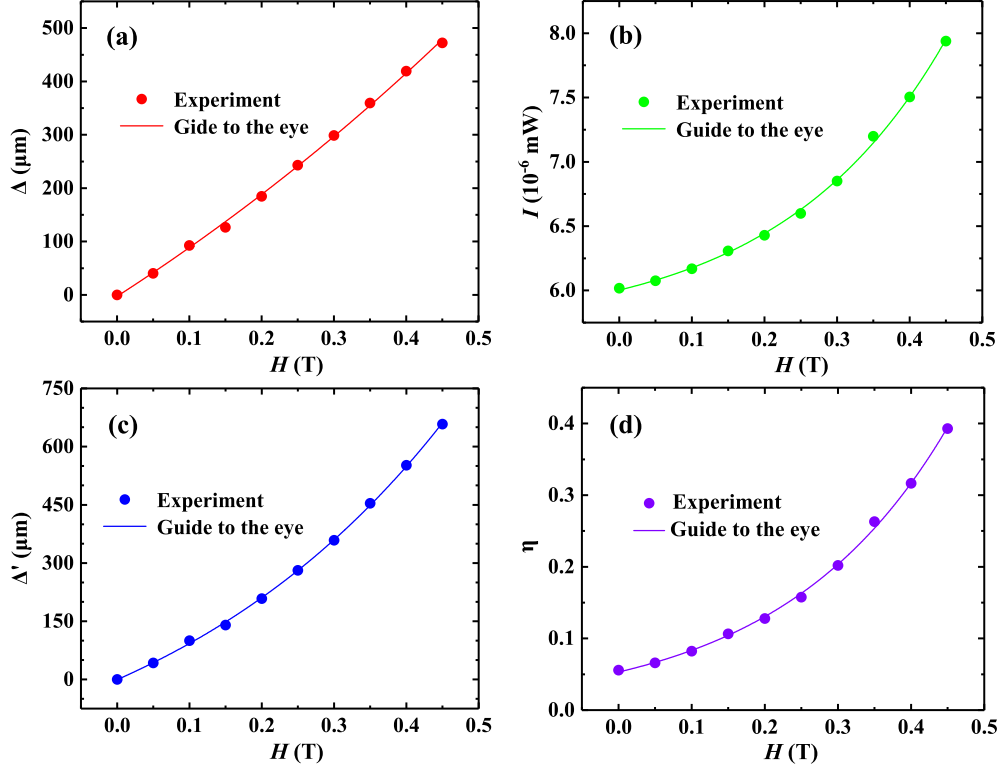


FIG. 4: The dependence of the pointers and the intensity of the magnetic field. (a) and (b) are the experiment results for the measurement of  $\Delta$  and  $I$ , under room temperature. (c) and (d) show the two new pointers  $\Delta'$  and  $\eta$  calculated by the measurement results. The scatters are the average values of the measurement, and the curves are the guides to the eye.

are shown in Fig.5(a). It can be seen that both of the two parameters increase with the increasing of  $H$ . The measurement precision of these two parameters can be evaluated by

$$S_{\theta_K} = \frac{\partial \theta_K}{\partial \Delta'} S_{\Delta'}, \quad (18)$$

$$S_{\epsilon_K} = \sqrt{\left(\frac{\partial \epsilon_K}{\partial \Delta'} S_{\Delta'}\right)^2 + \left(\frac{\partial \epsilon_K}{\partial \eta} S_{\eta}\right)^2}, \quad (19)$$

where  $S_{\Delta'}$  and  $S_{\eta}$  are the standard deviations of  $\Delta'$  and  $\eta$ , respectively. In this experiment, the measurement precision of  $\theta_K$  and  $\epsilon_K$  is in  $10^{-4}$  deg.

The complex magneto-optical constant  $Q = Q_0 \exp(-iq)$ , whose magnitude  $Q_0$  is proportional to the magnetization intensity [1], is also obtained. Where  $q$  is the phase. From Eq.(6),  $Q$  can be calculated by

$$Q = \frac{(n_1^2 - n_0^2)(\epsilon_K - i\theta_K)}{n_0 n_1 m_z}. \quad (20)$$

Since the plane of the Ni-Fe film is isotropic, and the applied magnetic field is normal to the film surface, we assume  $m_z = 1$  during the whole measurement process. The refractive indices of  $n_0$  and  $n_1$  are 1 and  $1.26 - 0.44i$ , respectively, where  $n_1$  is measured by the ellipsometer. We depict the dependence of  $Q$  and  $H$ , as shown in Fig.5(b).  $Q_0$  intuitively shows the

magnetization performance perpendicular to the film surface, while  $q$  remains a constant.

#### IV. CONCLUSION

In summary, we propose a method to measure the complex PMOKE using weak measurement. The beam is reflected normally from the magnetic sample, where the detected signal is purely given by PMOKE. The beam is then reflected obliquely from a prism surface to induce the spin splitting, which is employed as the weak coupling. It solves the problem that the traditional setup of MOKE using weak measurement can't be used to measure the pure PMOKE, for the reason that the spin splitting only exists with the oblique incidence. By introducing two new pointers,  $\Delta'$  and  $\eta$ , we realize the simultaneous measurement of  $\theta_K$  and  $\epsilon_K$  with the precision of  $10^{-4}$  deg, which addressed the problem that these two MOKE parameters have to be measured separately using traditional methods. According to the experiment results, the complex magneto-optical constant  $Q$  is also obtained. It is worthy noting that a higher measurement precision could be further achieved by employing the incident angle around Brewster's angle, and combing with the noise reduction techniques such as the lock-in amplifier and the squeezed light technique. This work has the value for the measurement of the complex PMOKE with high-efficiency and high-precision, and for the development

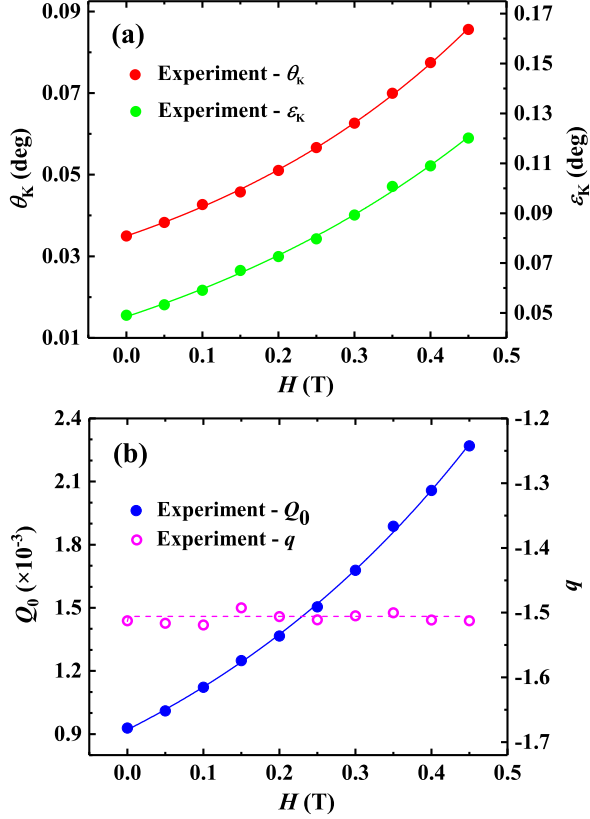


FIG. 5: The dependence of the complex MOKE parameters and the intensity of the magnetic field. (a)  $\theta_K$  and  $\epsilon_K$ , (b)  $Q_0$  and  $q$ . The scatters are the calculated results according to  $\Delta'$  and  $\eta$ , and the curves are the guides to the eye.

of the practical applications of the magneto-optical devices.

### ACKNOWLEDGMENTS

This work is supported by National Natural Science Foundation of China (61871451), Sichuan Science and Technology Program (2022YFG0166), and Joint Fund of Bijie City and Guizhou University of Engineering Science (BiJie science and Technology Union Contract [2023] No.16).

#### Appendix A: The theoretical spin splitting for the normal incidence

In this appendix, we take the SHEL induced by a non-magnetic medium with the incident state of  $|H\rangle$  as an example, to give a brief explanation of why the spin splitting is zero under the condition of  $\theta_i = 0$ .

Considering the incident light reflected from a sample, the

reflection coefficients  $r_p$  and  $r_s$  can be expressed by

$$r_p = \frac{n^2 \cos \theta_i - \sqrt{n^2 - \sin^2 \theta_i}}{n^2 \cos \theta_i + \sqrt{n^2 - \sin^2 \theta_i}}, \quad (\text{A1})$$

$$r_s = \frac{\cos \theta_i - \sqrt{n^2 - \sin^2 \theta_i}}{\cos \theta_i + \sqrt{n^2 - \sin^2 \theta_i}}, \quad (\text{A2})$$

where  $n$  is the refractive index of the medium. It can be seen that the spin splitting  $\delta = (1 + r_s/r_p) \cot \theta_i/k$  is mainly determined by  $n$  and  $\theta_i$ . When  $\theta_i = 0$ ,  $r_s/r_p \equiv -1$ . Thus  $\delta \equiv 0$ , where the spin-orbit coupling  $\exp(-i\delta\hat{\sigma}_y)$  is not exist. Therefore, the spin splitting induced by the measured sample can not be used as the weak coupling with the normal incidence. For magnetic medium and the incident light of arbitrary polarization state, the same conclude can be obtained.

#### Appendix B: Derivation of the calculation formula of the compensated $\Theta_K$

Considering the state of the incident polarization light in

$$|\psi_0\rangle = |H + \alpha\rangle = \begin{bmatrix} \cos \alpha \\ \sin \alpha \end{bmatrix}, \quad (\text{B1})$$

the state of the reflected light is described as

$$\begin{aligned} |\psi_r^1\rangle &= \mathfrak{R}_1 |H + \alpha\rangle \\ &= (r_{pp} \cos \alpha + r_{ps} \sin \alpha) |H\rangle + (r_{sp} \cos \alpha + r_{ss} \sin \alpha) |V\rangle. \end{aligned} \quad (\text{B2})$$

Since  $\alpha \ll 1$ , and  $r_{ss} \equiv -r_{pp}$  with the normal incidence,  $|\psi_r^1\rangle$  in the spin basis can be expressed by

$$\begin{aligned} |\psi_r^1\rangle &= \frac{1}{\sqrt{2}} [(r_{pp} \cos \alpha + r_{ps} \sin \alpha)(|+\rangle + |-\rangle) \\ &\quad - i(r_{sp} \cos \alpha - r_{ss} \sin \alpha)(|+\rangle - |-\rangle)] \\ &\approx \frac{r_{pp}}{\sqrt{2}} [1 \mp i(\frac{r_{sp}}{r_{pp}} - \alpha)] |\pm\rangle \\ &\approx \frac{r_{pp}}{\sqrt{2}} [e^{-i(\theta_K - \alpha) - \epsilon_K} |+\rangle + e^{i(\theta_K - \alpha) + \epsilon_K} |-\rangle]. \end{aligned} \quad (\text{B3})$$

By comparing to Eq.(4), we can see that the measured rotation angle is compensated by  $\alpha$ . In this case, the expressions of the two new pointers are changed to

$$\Delta' |_{\theta_K} = \frac{I |_{\theta_K, \epsilon_K} - I |_{\theta_K=0, \epsilon_K=0}}{I |_{\theta_K=0, \epsilon_K=0}} \Delta \approx \frac{2zr_s}{k\delta r_p} (\theta_K - \alpha), \quad (\text{B4})$$

$$\eta |_{\theta_K, \epsilon_K} = \frac{I |_{\theta_K, \epsilon_K} - I |_{\theta_K=0, \epsilon_K=0}}{I |_{\theta_K=0, \epsilon_K=0}} \approx \frac{r_s^2 w^2}{r_p^2 \delta^2} [(\theta_K - \alpha)^2 + \epsilon_K^2]. \quad (\text{B5})$$

Thus, the two parts of  $\Theta_K$  can be calculated by

$$\theta_K |_{\Delta'} = \frac{k\delta r_p}{2zr_s} \Delta' + \alpha, \quad (\text{B6})$$

$$\varepsilon_K|\Delta', \eta = \sqrt{\frac{r_p^2 \delta^2}{r_s^2 w^2} \eta - \left(\frac{k \delta r_p}{2z r_s} \Delta'\right)^2}. \quad (\text{B7})$$

- 
- [1] Z. J. Yang and M. R. Scheinfein, Combined three-axis surface magneto-optical Kerr effects in the study of surface and ultrathin-film magnetism, *Journal of Applied Physics* **74**, 6810 (1993).
- [2] C. You and S. Shin, Generalized analytic formulae for magneto-optical Kerr effects, *Journal of Applied Physics* **84**, 10.1063/1.368058 (1998).
- [3] R. A. Hajjar, F. L. Zhou, and M. Mansuripur, Magneto-optical measurement of anisotropy energy constants on amorphous rare-earth transition-metal alloys, *Journal of Applied Physics* **67**, 5328 (1990).
- [4] D. Weller, Y. Wu, J. Stöhr, M. G. Samant, B. D. Hermsmeier, and C. Chappert, Orbital magnetic moments of Co in multilayers with perpendicular magnetic anisotropy, *Phys. Rev. B* **49**, 12888 (1994).
- [5] T. Li, Q. Wang, A. Taallah, S. Zhang, T. Yu, and Z. Zhang, Measurement of the magnetic properties of thin films based on the spin Hall effect of light, *Optics Express* **28**, 29086 (2020).
- [6] Q. Wang, T. Li, L. Luo, Y. He, X. Liu, Z. Li, Z. Zhang, and J. Du, Measurement of hysteresis loop based on weak measurement, *Opt. Lett.* **45**, 1075 (2020).
- [7] L. Luo, T. Li, Y. Jiang, L. Fang, B. Liu, and Z. Zhang, Estimation of Kerr angle based on weak measurement with two pointers, *Opt. Express* **31**, 14432 (2023).
- [8] T. Li, L. Luo, X. Li, M. T. Dove, S. Zhang, J. He, and Z. Zhang, Observation of the mixed magneto-optical Kerr effects using weak measurement, *Opt. Express* **31**, 24469 (2023).
- [9] Y. Aharonov, D. Z. Albert, and L. Vaidman, How the result of a measurement of a component of the spin of a spin-1/2 particle can turn out to be 100, *Phys. Rev. Lett.* **60**, 1351 (1988).
- [10] O. Hosten and P. Kwiat, Observation of the spin Hall effect of light via weak measurements, *Science* **319**, 787 (2008).
- [11] X. Zhou, Z. Xiao, H. Luo, and S. Wen, Experimental observation of the spin Hall effect of light on a nanometal film via weak measurements, *Phys. Rev. A* **85**, 043809 (2012).
- [12] X. Ling, Z. Zhang, Z. Dai, Z. Wang, H. Luo, and L. Zhou, Photonic spin-Hall effect at generic interfaces, *Laser & Photonics Reviews*, 2200783 (2023).
- [13] H. Chen, G. Liu, S. Zhang, Y. Zhong, J. Yu, Z. Chen, and W. Zhu, Spin Hall effect of nonlinear photons, *Laser & Photonics Reviews*, 2200681 (2023).
- [14] D. J. Starling, P. B. Dixon, A. N. Jordan, and J. C. Howell, Precision frequency measurements with interferometric weak values, *Phys. Rev. A* **82**, 063822 (2010).
- [15] Y. Liu, Y. Zhang, Z. Xu, L. Zhou, Y. Zou, B. Zhang, and Z. Hu, Ultra-low noise phase measurement of fiber optic sensors via weak value amplification, *Optics Express* **30** (2022).
- [16] X.-Y. Xu, Y. Kedem, K. Sun, L. Vaidman, C.-F. Li, and G.-C. Guo, Phase estimation with weak measurement using a white light source, *Phys. Rev. Lett.* **111**, 033604 (2013).
- [17] R. Wang, S. He, and H. Luo, Photonic spin-Hall differential microscopy, *Phys. Rev. Appl.* **18**, 044016 (2022).
- [18] D. Li, T. Guan, F. Liu, A. Yang, Y. He, Q. He, Z. Shen, and M. Xin, Optical rotation based chirality detection of enantiomers via weak measurement in frequency domain, *Appl. Phys. Lett.* **112**, 213701 (2018).
- [19] J. Xiao, T. Tang, X. Liang, K. Liu, Y. Tang, J. Li, and C. Li, Chirality and concentration detection of biomolecules based on spin Hall effect of light, *Physics Letters A* **416**, 127692 (2021).
- [20] R. Wang, J. Zhou, K. Zeng, S. Chen, X. Ling, W. Shu, H. Luo, and S. Wen, Ultrasensitive and real-time detection of chemical reaction rate based on the photonic spin Hall effect, *APL Photonics* **5**, 016105 (2020).
- [21] R. Zhao, X. Wang, P. Wang, X. Wu, X. Fang, Y. Zhang, and S. Li, Experimentally monitoring of the rapid biomolecular hydrolysis reaction with optical weak measurement, *Laser Physics* **32**, 125201 (2022).
- [22] O. S. Magaña-Loaiza, M. Mirhosseini, B. Rodenburg, and R. W. Boyd, Amplification of angular rotations using weak measurements, *Phys. Rev. Lett.* **112**, 200401 (2014).
- [23] S. Chen, X. Zhou, X. Ling, W. Shu, H. Luo, and S. Wen, Measurement of the optical constants of monolayer MoS<sub>2</sub> via the photonic spin Hall effect, *Applied Physics Letters* **118**, 111104 (2021).
- [24] X. Zhou, L. Sheng, and X. Ling, Photonic spin Hall effect enabled refractive index sensor using weak measurements, *Scientific Reports* **8**, 1221 (2018).
- [25] S. Chen, X. Ling, W. Shu, H. Luo, and S. Wen, Precision measurement of the optical conductivity of atomically thin crystals via the photonic spin hall effect, *Phys. Rev. Applied* **13**, 014057 (2020).
- [26] T. Tang, Y. Tang, L. Bi, T. Kang, X. Liang, J. Qin, J. Li, L. Luo, and C. Li, Highly sensitive real-time detection of phase change process based on photonic spin Hall effect, *Applied Physics Letters* **120**, 191105 (2022).
- [27] Q. Qiu, Z and S. D. Bader, Surface magneto-optic Kerr effect, *Rev. Sci. Instrum.* **71**, 1243 (2000).
- [28] Y. He, L. Luo, L. Xie, J. Shao, Y. Liu, J. You, Y. Ye, and Z. Zhang, Detection of magneto-optical kerr signals via weak measurement with frequency pointer, *Opt. Lett.* **46**, 4140 (2021).
- [29] H. Luo, X. Zhou, W. Shu, S. Wen, and D. Fan, Enhanced and switchable spin hall effect of light near the brewster angle on reflection, *Phys. Rev. A* **84**, 043806 (2011).